

Copyright  
by  
Alina Arkadievna Blinova  
2015

The Thesis Committee for Alina Arkadievna Blinova  
Certifies that this is the approved version of the following thesis:

**Simulating the Magnetic Implosion of an Atomic  
Hydrogen Cloud for the Measurement of Three-Body  
Association**

APPROVED BY

SUPERVISING COMMITTEE:

---

Mark Raizen, Supervisor

---

Greg Sitz

**Simulating the Magnetic Implosion of an Atomic  
Hydrogen Cloud for the Measurement of Three-Body  
Association**

by

**Alina Arkadievna Blinova, A.B.**

**THESIS**

Presented to the Faculty of the Graduate School of

The University of Texas at Austin

in Partial Fulfillment

of the Requirements

for the Degree of

**MASTER OF ARTS**

THE UNIVERSITY OF TEXAS AT AUSTIN

August 2015

*To my astro parents*

## Acknowledgments

I would like to thank my advisor, Mark Raizen, for giving me the opportunity to work with him, and for being so helpful, patient and understanding every step of the way. The collegial atmosphere that Mark fosters in his group has been a great help in the making of this work, and I would like to thank all the members of the Raizen Lab for their help and their time. I also want to thank Greg Sitz for taking the time to review this thesis.

I want to thank Malcolm Boshier and Eddy Timmermans of Los Alamos National Laboratory for their support and encouragement, without which I would not be where I am today. My parents, Marina Romanova and Richard Lovelace, have always been an inspiration, and I would like to thank them for their understanding, their help and their endless patience. Finally, I want to thank my sister and all my friends for being there for me in many times of need.

# Simulating the Magnetic Implosion of an Atomic Hydrogen Cloud for the Measurement of Three-Body Association

Alina Arkadievna Blinova, M.A.  
The University of Texas at Austin, 2015

Supervisor: Mark Raizen

Three-body association (TBA) of hydrogen is the process by which three hydrogen atoms combine to form a hydrogen molecule and a free atom. The TBA reaction rate is not known precisely, yet its value plays a crucial role in the formation of the first stars. We propose an experiment to measure the TBA of hydrogen using a magnetic field to implode a cloud of atomic hydrogen to achieve high densities.

In this work I present the results of a numerical simulation for the idealized case of non-interacting, point-like hydrogen atoms in a hexapole magnetic field. The results show that in this approximation, high atomic densities can be reached. Using existing TBA rate estimates, I show that observation of TBA on short time-scales is feasible with the range of atomic densities available in the proposed experiment. For a more accurate simulation, a closer look at atom-atom interactions and the thermal evolution of the cloud is needed.

# Table of Contents

<b>Acknowledgments</b>	<b>v</b>
<b>Abstract</b>	<b>vi</b>
<b>List of Tables</b>	<b>ix</b>
<b>List of Figures</b>	<b>x</b>
<b>Chapter 1. Introduction</b>	<b>1</b>
1.1 Motivation . . . . .	1
1.2 Previous work . . . . .	2
1.3 Goal of this thesis . . . . .	4
<b>Chapter 2. Proposed Experiment</b>	<b>5</b>
2.1 Cooling and trapping of atomic hydrogen . . . . .	5
2.1.1 Previous efforts . . . . .	6
2.1.2 Efforts in our lab . . . . .	7
2.2 Hexapole magnetic trap . . . . .	9
2.2.1 Why hexapole? . . . . .	10
2.2.2 Implosion . . . . .	11
2.3 Detection of H <sub>2</sub> . . . . .	12
<b>Chapter 3. Numerical Simulation</b>	<b>15</b>
3.1 Hydrogen in a magnetic field . . . . .	15
3.1.1 Hyperfine Structure of Hydrogen . . . . .	15
3.1.2 Zeeman effect on hyperfine structure . . . . .	16
3.1.2.1 Weak-field Zeeman effect . . . . .	18
3.1.2.2 Strong-field Zeeman effect . . . . .	19
3.2 Initial conditions . . . . .	20

3.3	Equations of motion . . . . .	22
3.4	Choosing the right kick strength . . . . .	23
3.5	Results . . . . .	24
3.5.1	Reaction temperature . . . . .	24
<b>Chapter 4.</b>	<b>Discussion</b>	<b>27</b>
4.1	Can we achieve densities that are high enough for TBA? . . .	28
4.1.1	Percent conversion . . . . .	29
4.2	Thermodynamics and secondary reactions . . . . .	36
4.2.1	Heating . . . . .	36
4.2.2	Cooling . . . . .	36
4.3	Concluding remarks . . . . .	38
	<b>Bibliography</b>	<b>39</b>

## List of Tables

3.1	Values of the half-period of oscillation, $T/2$ , as a function of the field strength constant, $\kappa$ . . . . .	24
3.2	Reaction temperatures, $T$ , calculated from the simulated motion of atoms at the time of implosion. $\kappa$ is the field strength and pulse duration is assumed to be $10 \mu s$ . The initial cloud temperature in this example is 10 nK, though the initial temperature has little effect on reaction temperature. . . . .	25
4.1	Hydrogen TBA rate constants as published by various authors. $T$ is the gas temperature in Kelvin. . . . .	28

# List of Figures

2.1	Color scale cross section of the magnetic field inside a hexapole trap. Dark blue denotes regions of low magnetic field and light blue denotes regions of high magnetic field. The thin black circles represent the current-carrying copper wires, arranged at the vertices of an imaginary hexagon. White circles show the direction of the current flow inside the wires. . . . .	9
2.2	Schematic of the implosion sequence. The orange sticks along the $z - axis$ represent the six hexapole trap wires. The small blue dots represent hydrogen atoms. The cloud image is taken from an actual simulation of implosion that is to-scale frame-to-frame, but not-to-scale with the hexapole wires. In this simulation example, there are $10^5$ atoms and they start with a distribution that is slightly oblong. Regardless of initial cloud shape, the atoms reach the center at the same time. The field strength is $\kappa = 10^5 \text{ T/m}^2$ and a pulse of duration $10 \mu\text{s}$ is imparted at time $t = 0$ . <b>a)</b> $t = 0$ : cloud before the magnetic kick <b>b)</b> $t = 100 \mu\text{s}$ <b>c)</b> $t = 160 \mu\text{s}$ <b>d)</b> $175 \mu\text{s}$ : $2 \mu\text{s}$ before final implosion	14
3.1	Hyperfine energy splitting of the ground state of hydrogen in the presence of an external magnetic field. Here $A = \Delta_{HFS}$ . When the field is weak, the $F=1$ state is triply degenerate. When the external field becomes comparable in strength to the hyperfine energy splitting, $\Delta_{HFS}$ , the degeneracy is lifted and the energy levels move further apart. <b>a</b> and <b>b</b> are high-field seeking states, while <b>c</b> and <b>d</b> are the low-field seekers that can be trapped with a static magnetic field. This image has been modified from the original by C. J. Foot [1]. . . . .	17
3.2	Initial cloud distribution used in our simulation. The cloud contains $10^6$ atoms in a Gaussian profile with standard deviations given in Equations 3.13, 3.14 and 3.15. Because the magnetic hexapole does not act in the $z - direction$ , the width of the cloud in the $z - direction$ does not affect the results. . . . .	21
3.3	Simulated cloud densities during implosion. $10^6$ atoms are given a $10 \mu\text{s}$ kick with $\kappa = 10^5 \text{ T/m}^2$ . Initial cloud temperatures are given. It can be seen that the initial cloud temperature has a significant effect on final density. . . . .	26

4.1	TBA rate constants based on published estimates. The constants are plotted for the temperature range: 10 nK - 300 K. The constant published by Abel is specifically for temperatures below 300 K. . . . .	29
4.2	The percent conversion of H into H <sub>2</sub> using $k_3$ expression of Abel et. al. The reaction temperature is assumed to be 10 mK, which corresponds to a 10 $\mu$ s kick with $\kappa = 10^5$ T/m <sup>2</sup> . . . . .	32
4.3	The percent conversion of H into H <sub>2</sub> using $k_3$ expression of Abel et. al. The reaction temperature is assumed to be 1 K, which corresponds to a 10 $\mu$ s kick with $\kappa = 10^6$ T/m <sup>2</sup> . . . . .	33
4.4	The percent conversion of H into H <sub>2</sub> using $k_3$ expression of Flower & Harris. The reaction temperature is assumed to be 10 mK, which corresponds to a 10 $\mu$ s kick with $\kappa = 10^5$ T/m <sup>2</sup>	34
4.5	The percent conversion of H into H <sub>2</sub> using $k_3$ expression of Flower & Harris. The reaction temperature is assumed to be 1 K, which corresponds to a 10 $\mu$ s kick with $\kappa = 10^6$ T/m <sup>2</sup> . . .	35

# Chapter 1

## Introduction

Three-body association (TBA) is the process by which three atoms combine to form a two-atom molecule and a free atom. The third atom is necessary to conserve energy and momentum in the reaction. For the case of hydrogen atoms, the TBA process can be represented as:



The TBA rate of hydrogen is of fundamental interest in many areas of science, including plasma physics, rocket propulsion, chemical dynamics and astrophysics [2].

### 1.1 Motivation

To date, the TBA rate of hydrogen is not known precisely, yet its value plays a significant role in the study of the early universe. The first stars (Population III stars) are thought to have originated from cosmological objects that formed from primordial gas. Primordial gas contained only the lightest elements, principally hydrogen and helium. The objects that became the first stars in the universe formed when the primordial cloud condensed and collapsed under its own gravity. As the density and temperature of the cloud

change, a multitude of chemical processes take place. The hydrodynamics simulations of Turk et. al.[3] showed that certain crucial details of the collapse depend strongly on the rate of formation of molecular hydrogen through TBA.

Uncertainty in the TBA rate of hydrogen propagates outward into our understanding of the development of the universe. Variations in the TBA rate lead to different outcomes of the mass-spectrum of the first stars [4]. Because the mass of a star determines what elements it will produce in its lifetime through nucleosynthesis, uncertainty in the TBA rate limits our understanding of the chemistry of the early universe [2].

The way the TBA process affects the temperature of the collapsing cloud is non-trivial. The hydrogen TBA reaction is exothermic and there is a chemical heating rate associated with formation of  $H_2$ . The energy corresponding to the binding energy of  $H_2$  is released each time a molecule is formed. Meanwhile, radiative line cooling from the de-excitation of highly-excited vibrational and rotational states of the newly-born  $H_2$  molecules is thought to be the dominant coolant in the primordial gas [4].

## 1.2 Previous work

Estimates for the TBA rate of hydrogen have been made both from theoretical and experimental work. Shock-tube measurements performed in the 1960's by Jacobts et. al.[5] is the main experimental work on which subsequent published TBA rate constants by Palla et. al.[4], Abel et. al.[6], and Flower & Harris[7] are based. These published rate coefficients agree reason-

ably well for high temperatures, but disagree by orders of magnitude for lower temperatures that are relevant for early star formation [3]. Temperatures that are pertinent to astrophysical models are  $\sim 200 - 2000$  K [8], while the measurements of Jacobs et. al. were performed over a temperature range of 2900 - 4700 K. Moreover, the actual measurement was performed for the reverse process, known as collisional dissociation (CD):



and the TBA rate constant was deduced based on the principle of microscopic reversibility.

The TBA rate constant of Palla et. al. is identical to that given in Jacobs et. al. Flower & Harris derived a different TBA rate constant but still based on the results of Jacobs et. al. Meanwhile, the expression for the TBA rate derived by Abel et. al. is based on an extrapolation of classical trajectory calculations of Orel et. al. [2], which were performed for temperatures below 300 K. A quantum mechanical calculation of TBA rate constants in the temperature range  $300 < T < 10000$  K was performed by Forrey [9]. Thus we have four different expressions for the hydrogen TBA rate constant.

The TBA rate of spin-polarized hydrogen in a magnetic field (3 - 9 T) has been measured [?], but this measurement is not at all relevant to the spin-unpolarized case of interest. Magnetic dipole interactions of the spin-polarized atoms suppress TBA at relatively high densities, making the spin-polarized gas a lot more stable. The highest density achieved under controlled conditions

with spin-polarized hydrogen was  $4.5 \times 10^{18} \text{ cm}^{-3}$  at 0.55 K [10] [11]. In fact, decades ago, spin-polarized atomic hydrogen was the first candidate considered for the realization of Bose-Einstein condensation.

### **1.3 Goal of this thesis**

The goal of this thesis is to shed some light on the feasibility of measuring the three-body association rate of spin-neutral hydrogen. In this thesis I first lay out the experiment, proposed by Mark G. Raizen, for measuring the hydrogen TBA rate. I then describe and present the results of a numerical simulation of the atomic cloud. Finally, I discuss the results of the simulation, taking into account the published TBA rate coefficients. I conclude with the take-away lessons as well as suggestions for the experiment and future simulations.

# Chapter 2

## Proposed Experiment

To measure the TBA rate of hydrogen, control is needed over certain gas parameters, notably density and temperature. This is not so easily achieved. Atomic hydrogen gas is highly unstable due to TBA. Thus, atomic hydrogen can only be cooled and condensed when it is spin-polarized in a magnetic field. Hydrogen cannot be optically cooled and trapped like the alkali metals because the laser needed to drive the hydrogen  $1S \rightarrow 2P$  transition is not available. Thus alternative cooling methods are needed, which are briefly outlined below.

In this Chapter I describe the proposed experiment for measuring the TBA rate of hydrogen. A key part of the experiment is the hexapole magnetic trap that creates a harmonic potential for the trapped atoms. A pulse from such a trap implodes the cloud on itself and creates high atom densities in the center.

### 2.1 Cooling and trapping of atomic hydrogen

Our proposed experiment relies on the cold and dense initial conditions of the hydrogen cloud. We plan to implode the cloud in such a way that the atoms arrive at the center of the trap at the same time. In this way, under

ideal conditions, a very high density could be reached at the center, limited only by collisional processes. However, if there is thermal motion in the cloud prior to the implosion, then the random initial velocities of the atoms will preclude them from traveling directly into the center of the trap at just the right speed. The cloud also needs to be at the right density so the TBA can be observed. Thus the first step of the experiment is to confine and cool a cloud of hydrogen atoms.

### 2.1.1 Previous efforts

The hydrogen atom has evaded cooling and capture by the powerful techniques of laser cooling and trapping. This is because hydrogen is fundamentally different from the other atomic species that have been optically cooled and trapped. Hydrogen has a very low mass, making its photon recoil energy so large that a hydrogen cloud cannot be optically cooled below a few millikelvin [12]. Moreover, optical cooling of hydrogen faces a pragmatic barrier. The  $1S \rightarrow 2S$  transition of hydrogen requires a laser of 121 nm, which is not available. With the use of frequency doubling in nonlinear media, it is possible to build a laser at 243 nm to drive the transition with two photons. But this technique is further complicated by the fact that the hydrogen 2S state is metastable with a lifetime approaching 1 second, so the necessary cycling in this transition has to be induced by quenching [13]. Hydrogen also has an anomalously small elastic scattering cross section ( $0.648 \text{ \AA}$ ), which slows and eventually limits the evaporative cooling rate.

Efforts to create and stabilize condensed atomic hydrogen began in the 1970's and were lead by Silvera and Walraven [14] and by Kleppner and Greytak [15]. They confined and stabilized atomic hydrogen in a magnetic trap with a high bias magnetic field (up to 7 T) and at low temperatures (average of 270 mK). The hydrogen had to be cooled with a cryogenic filling technique, conceived by Silvera and Walraven, exploiting interatomic collisions and heat exchange with liquid helium covered surfaces. Because superfluid helium has a very weak adsorption potential for hydrogen, it proved to be vital for stabilization [14]. However, adsorption on the helium-coated walls still existed and this, together with subsequent TBA on the wall surfaces, limited the lifetime and temperature of the gas [16].

Further efforts [17] in confinement of spin-polarized atomic hydrogen lead to the thermal decoupling of the gas from the walls and very long (tens of minutes) lifetimes of the trapped gas, with the gas temperature at approximately 40 mK. The long lifetime of the gas allowed for the application of evaporative cooling techniques [18], which shortly lead to the first hydrogen BEC [19]. The BEC transition was observed to occur at a temperature of approximately  $T = 50 \mu\text{K}$  and number density of  $1.8 \times 10^{14} \text{ cm}^{-3}$  [19]. At such a density, spin-unpolarized hydrogen is not stable.

### **2.1.2 Efforts in our lab**

In our lab we are currently building a new magnetic atom slower, or coilgun, that will have the capacity to cool any paramagnetic atomic species,

including hydrogen. An earlier version of this slower was built in our lab 8 years prior. The coilgun emits a highly-compressed "bullet" of He or Ne gas through a small aperture. Noble gas bullets shoot out, at supersonic speeds, forming a supersonic beam. The beam is directed into a long tube lined with magnetic coils. Many other atomic species, including hydrogen and lithium, can be entrained in the beam. By correctly timing current pulses in the coils, the induced magnetic fields create a series of potential "hills" for the atoms to climb, thus taking away their kinetic energy and slowing them down. In the moving frame of the atoms, the gas temperature is in the tens of millikelvin. When the atoms are finally brought to a halt they are cold and can be trapped in a static magnetic trap. Details of the coilgun can be found in [20].

Hydrogen has a very small scattering length, so thermalization of the gas is slow. To overcome this disadvantage we plan to have the hydrogen entrained in lithium for the duration of the cooling process, beginning with the supersonic beam. It has been shown that cooling of hydrogen can be enhanced through collisions with  ${}^7\text{Li}$  [21]. For further cooling, we can employ several methods, including evaporative cooling and MOP [22] cooling. Through evaporative cooling, William and Kleppner [12] were able to cool  $10^{14}$  atoms at 40 mK down to  $100 \mu\text{K}$  at the price of losing a fraction of the cloud and ending with  $10^{11}$  atoms.

In what follows we assume we can obtain at least  $10^{10}$  atoms cooled to quantum degeneracy.

## 2.2 Hexapole magnetic trap

Once a cloud of quantum degenerate hydrogen is obtained, it can be loaded into a hexapole magnetic trap. The hexapole trap consists of six parallel wires running along the  $z$ -axis, equidistant from each other and placed at the vertices of an imaginary hexagon. When alternating electric currents are sent through the wires a hexapole magnetic field, with cylindrical symmetry about the  $z$ -axis, is produced. The magnitude of the magnetic field increases quadratically with the radial distance,  $\rho$ , from the  $z$ -axis. A finite-element calculation of the magnetic field profile is shown in Figure 2.1

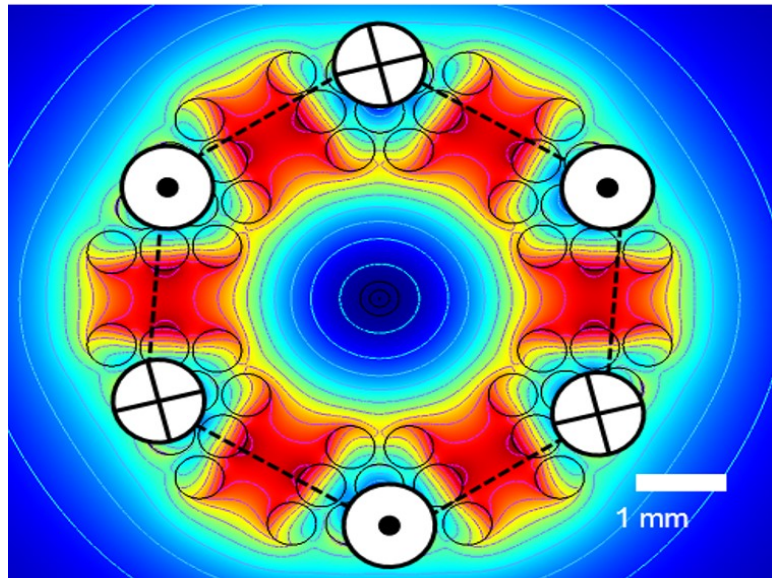


Figure 2.1: Color scale cross section of the magnetic field inside a hexapole trap. Dark blue denotes regions of low magnetic field and light blue denotes regions of high magnetic field. The thin black circles represent the current-carrying copper wires, arranged at the vertices of an imaginary hexagon. White circles show the direction of the current flow inside the wires.

The quadratic dependence of the field is made evident if we expand the magnetostatic potential in multipole terms of the form [23]:

$$\Phi_n \propto \rho^{n-1} \quad (2.1)$$

Near the  $z$  – *axis* the lowest multipole,  $\Phi_3$ , dominates and  $B \propto |\nabla\Phi_3| \propto \rho^2$ .

The hexapole magnetic field can be written as:

$$\mathbf{B} = \frac{1}{2}\kappa\rho^2\hat{\boldsymbol{\rho}} \quad (2.2)$$

where  $\kappa$  characterizes the field strength and has units of T/m<sup>2</sup>.

In our lab, the hexapole trap has been used as a pulsed magnetic lens in a neutral atom imaging experiment [24]. In order to produce large field constants  $\kappa = 10^4 - 10^6$  T/m<sup>2</sup>, the dimensions of the hexapole electromagnet are made to be small, with the spacing between the wires on the order of a few millimeters.

### 2.2.1 Why hexapole?

The hexapole magnetic trap is crucial to the experiment because it produces a harmonic potential for the trapped atoms. As will be shown in Section 3.1, the interaction energy,  $E_{int}$ , between a trapped hydrogen atom and an external magnetic field,  $B_{ext}$ , is given by:

$$E_{int} = \mu_B B_{ext} \quad (2.3)$$

where  $\mu_B$  is the Bohr magneton. Using Equation 2.2 we see that  $E_{int} \propto \rho^2$ , so the atom experiences a radial harmonic potential and its motion within the hexapole trap can be described in terms of a simple harmonic oscillator.

The period of oscillation is an intrinsic property of the simple harmonic oscillator. It is independent of the initial conditions. As will be shown in Section 3.3, the oscillation frequency of a hydrogen atom inside the hexapole trap is:

$$\omega = \sqrt{\frac{\mu_B \kappa}{m}} \quad (2.4)$$

where  $m$  is the mass of the hydrogen atom. This means that regardless of where the atoms start out with respect to the trap center, when the hexapole field is switched on, the atoms will begin to oscillate, crossing the center of the trap at the same time. It is at the moment of the first crossing that we expect to produce high atomic densities and to observe TBA.

### 2.2.2 Implosion

In order to observe the spin-neutral TBA reaction, the magnetic field needs to be switched off before the atoms reach the critical density at which  $H_2$  production becomes observable. When the hexapole trap is suddenly switched on, the atomic spins will align with the field and will point in the radial direction. Once the field is switched off the spins will remain frozen in this configuration. Due to symmetry, the spins average out to 0.

The pulsed magnetic hexapole trap would give the atoms just a momentary "kick" toward the center. To achieve this it is necessary to produce very short current pulses through the hexapole wire coils. Magnetic pulse durations of less than  $10 \mu s$  are feasible. In our lab, such short pulses have been employed in the coilgun (see Section 2.1.2), where a high current pulse is

produced by allowing a capacitor to discharge across the coil. Integrated gate bipolar transistors act as fast switches [25].

Once the field is switched off the atoms continue to move toward the center at a constant velocity. We simulated this implosion sequence and the results can be found in Chapter 3. A schematic of the implosion sequence is shown in Figure 2.2.

### 2.3 Detection of H<sub>2</sub>

H<sub>2</sub> molecules can be detected using Resonant Excitation MultiPhoton Ionization (REMPI) [26]. REMPI works by ionizing the hydrogen molecules into H<sub>2</sub><sup>+</sup>, which are readily detected with the use of a bias electric field to deflect the motion of the charged particles. The REMPI method can detect only one ro-vibrational level of H<sub>2</sub> at a time. TBA calculations using resonance complex theory carried out by Orel [2] show that the initial vibrational/rotational distribution peaks in the highest bound states of the molecule. The average vibrational level is high. The initial distribution of rotational/vibrational states will be greatly changed by subsequent collisions as the highly-excited states are not stable. Subsequent collisions will cause molecular line transitions.

According to Savin [8] a rough estimate for the required atomic hydrogen number density is given by:

$$n_H \sim \left( \frac{S}{k_3 V} \right)^{1/3} \quad (2.5)$$

where S is the signal rate,  $k_3$  is the TBA rate coefficient, and V is the detected

interaction volume. In the lab of Greg O. Sitz at the University of Texas at Austin, REMPI on  $\text{H}_2$  can detect about  $10^6$  molecules per  $\text{cm}^3$  per quantum state. This density would yield about 1 ion in a laser pulse. The volume probed is roughly a cylinder about  $20 \mu\text{m}$  in diameter and a few mm long [27]. The TBA rate coefficient,  $\kappa_3$  is not known precisely, especially for low temperatures, but published rate constants exist and are used in Chapter 4 to discuss simulation results. Ultimately, we want to know what kind of atomic densities we need to achieve in the hexapole trap to observe the TBA of hydrogen.

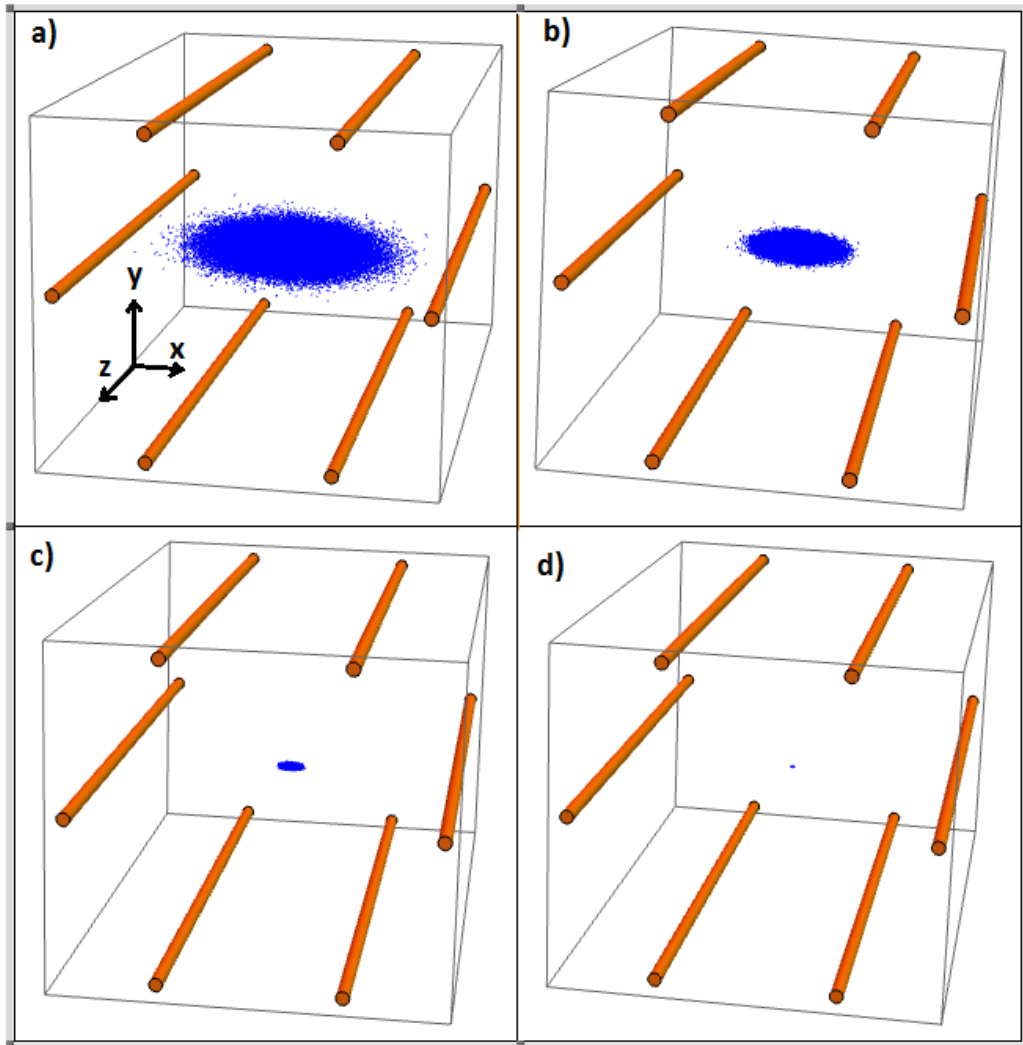


Figure 2.2: Schematic of the implosion sequence. The orange sticks along the  $z$  - axis represent the six hexapole trap wires. The small blue dots represent hydrogen atoms. The cloud image is taken from an actual simulation of implosion that is to-scale frame-to-frame, but not-to-scale with the hexapole wires. In this simulation example, there are  $10^5$  atoms and they start with a distribution that is slightly oblong. Regardless of initial cloud shape, the atoms reach the center at the same time. The field strength is  $\kappa = 10^5$  T/m<sup>2</sup> and a pulse of duration  $10 \mu\text{s}$  is imparted at time  $t = 0$ . **a)**  $t = 0$ : cloud before the magnetic kick **b)**  $t = 100 \mu\text{s}$  **c)**  $t = 160 \mu\text{s}$  **d)**  $175 \mu\text{s}$ :  $2 \mu\text{s}$  before final implosion

## Chapter 3

### Numerical Simulation

We simulate the hydrogen atoms as noninteracting, classical point particles. We start with a quantum degenerate gas of atomic hydrogen having a number density of  $10^{14} \text{ cm}^{-3}$ . We expect an atom number of around  $10^{10}$ . Simulating this many particles would take a very long time, so taking advantage of the fact that we are really concerned with particle density, not number, we simulated  $10^6$  particles. Parameters such as field strength, magnetic kick duration, initial cloud density, temperature and shape, can all be varied.

For the simulation run presented in this thesis, the particles start out in a pencil-shaped cloud and are given a  $10 \mu\text{s}$  hexapole kick. The final density is calculated inside a  $1 \mu\text{m}$  spherical core. We show that atom densities of  $10^{16} \text{ cm}^{-3}$  are attainable inside the core.

#### 3.1 Hydrogen in a magnetic field

##### 3.1.1 Hyperfine Structure of Hydrogen

Hyperfine structure is a result of the interaction between the dipole moment of the atomic nucleus and the dipole moment of the surrounding electrons. Electrons inside an atom create an internal magnetic flux density,

$\mathbf{B}_e$ , that is a result of an electron's spin dipole moment and, for states with  $l \neq 0$ , the electron's orbital motion. For atoms that have a nuclear spin, the nuclear magnetic moment is given by  $\mu_{\mathbf{I}} = g_I \mu_N \mathbf{I}$ , where  $g_I$  is the nuclear g-factor and  $\mu_N$  the nuclear magneton. The interaction Hamiltonian between the nuclear magnetic moment and the internal field is:

$$H_{HFS} = -\mu_{\mathbf{I}} \cdot \mathbf{B}_e \quad (3.1)$$

This interaction gives rise to hyperfine structure.

When considering hyperfine structure, we need to consider the total angular momentum operator of the atom,  $\mathbf{F} = \mathbf{I} + \mathbf{J}$ , with  $\mathbf{J} = \mathbf{L} + \mathbf{S}$ . A hydrogen atom in the ground state  $1s^2S_{1/2}$  has quantum numbers  $L = 0$ ,  $S = 1/2$ , and  $I = 1/2$ . Thus the hydrogen ground state is split into two states: the triplet,  $F = 1$ , state, and the singlet,  $F = 0$ , state. In the  $F = 1$  state the nuclear spin is parallel to the electron spin. In the  $F = 0$  state the spins are antiparallel. The two states are separated by the hyperfine interaction energy,  $\Delta_{HFS}$ , corresponding to the famous 21 cm hydrogen line.

### 3.1.2 Zeeman effect on hyperfine structure

To simulate a cloud of hydrogen atoms in a magnetic trap we need to know the interaction energy between the atom and the magnetic field. Because an external magnetic field,  $\mathbf{B}_e$ , affects the hyperfine states of hydrogen, we need to consider the Zeeman effect on hyperfine structure.

An external magnetic field lifts the degeneracy in the  $F = 1$  state and

shifts the  $F = 0$  state downward. The  $F = 1$  state is split into three levels, with the total angular momentum projection  $M_F = -1, 0, 1$ . The energy splitting is a function of the field strength, and the levels move further apart as the field increases. This is shown in the diagram in Figure 3.1.

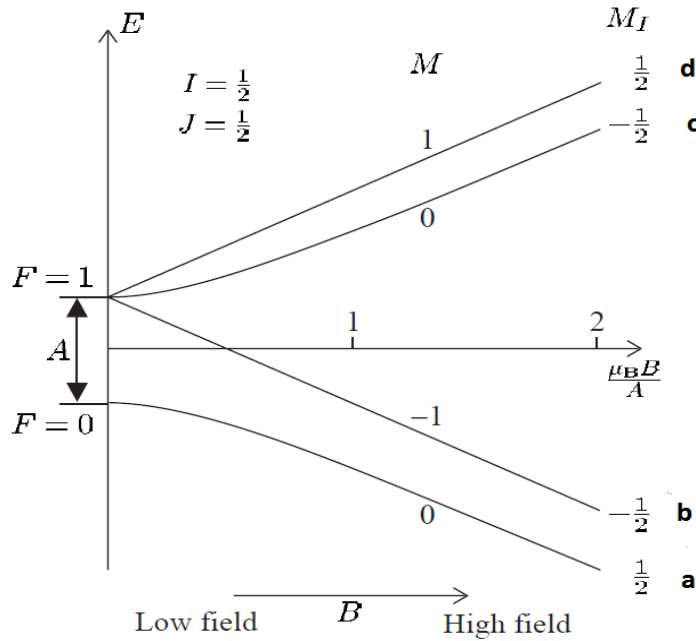


Figure 3.1: Hyperfine energy splitting of the ground state of hydrogen in the presence of an external magnetic field. Here  $A = \Delta_{HFS}$ . When the field is weak, the  $F=1$  state is triply degenerate. When the external field becomes comparable in strength to the hyperfine energy splitting,  $\Delta_{HFS}$ , the degeneracy is lifted and the energy levels move further apart. **a** and **b** are high-field seeking states, while **c** and **d** are the low-field seekers that can be trapped with a static magnetic field. This image has been modified from the original by C. J. Foot [1].

To obtain the interaction energy between an atom and the external

field, we start with the interaction Hamiltonian:

$$H_{int} = -\mu_{\text{atom}} \cdot \mathbf{B}_e \quad (3.2)$$

where  $\mu_{\text{atom}}$  is the atom's magnetic moment. It has orbital, spin and nuclear contributions:

$$\mu_{\text{atom}} = -g_J \mu_B \mathbf{J} + g_I \mu_N \mathbf{I} \quad (3.3)$$

Here,  $g_I$  is the nuclear g-factor,  $\mu_B$  is the Bohr magneton, and  $\mu_N$  the nuclear magneton.  $g_J$  is the Landé g-factor and is given by:

$$g_J = \frac{3}{2} + \frac{S(S+1) - L(L+1)}{2J(J+1)} \quad (3.4)$$

Because  $\mu_N \ll \mu_B$ , the second term in Equation 3.3 can be ignored, and the interaction Hamiltonian reduces to:

$$H_{int} = g_J \mu_B \mathbf{J} \cdot \mathbf{B}_e \quad (3.5)$$

When the interaction energy with the external field is weaker than the hyperfine interaction, that is, when  $\mu_B B_e < \Delta_{HFS}$ , then  $H_{int}$  is treated as a perturbation to the eigenstates defined by  $|F, M_F\rangle$ . This is the weak-field regime. In the strong-field regime, where  $\mu_B B_e > \Delta_{HFS}$ , the interaction energy is evaluated with respect to the  $|M_J, M_I\rangle$  eigenstates.

### 3.1.2.1 Weak-field Zeeman effect

When the hyperfine interaction dominates, the interaction with the external field is treated as a perturbation relative to the hyperfine states.

Thus  $F$  and  $M_F$  are good quantum numbers. Using Equation 3.5 and taking the projection of the magnetic moments along  $\mathbf{F}$  yields:

$$E_{int} = g_F \mu_B B M_F \quad (3.6)$$

with  $g_F$  given by:

$$g_F = \frac{F(F+1) + J(J+1) - I(I+1)}{2F(F+1)} g_J \quad (3.7)$$

Thus, to first order in the weak-field limit, only  $\mathbf{b}$  and  $\mathbf{d}$  states interact with the external field. The interaction energy is given by:

$$E_{int} = \pm \mu_B B \quad (3.8)$$

### 3.1.2.2 Strong-field Zeeman effect

When the interaction energy is greater than than  $\Delta_{HFS}$ ,  $\mathbf{J}$  precesses about  $\mathbf{B}$  and  $M_I$  and  $M_J$  become the good quantum numbers. The strong-field interaction energy is given by:[1]

$$E_{int} = g_J \mu_B B M_J + \Delta_{HFS} M_I M_J \quad (3.9)$$

Thus, in the strong-field limit the degeneracy is lifted and there are four distinct energy levels of the hydrogen ground state. The interaction energy is given by:

$$E_{int} = \pm \mu_B B \pm \Delta_{HFS}/4 \quad (3.10)$$

By definition, in the strong-field limit  $\Delta_{HFS} < \mu_B B$  and the  $\Delta_{HFS}/4$  term can be ignored. For the simulation we assume that the atoms are in the

**d** state and thus experience the same interaction energy in the strong- and weak-field limits:

$$E_{int} = \mu_B B \quad (3.11)$$

### 3.2 Initial conditions

Each particle is given an initial position, according to a 3-dimensional Gaussian distribution about the center of the trap, and an initial velocity, according to the Maxwell-Boltzmann distribution:

$$f(v) = \sqrt{\left(\frac{m}{2\pi kT}\right)^3} 4\pi v^2 e^{-\frac{mv^2}{2kT}}. \quad (3.12)$$

$f(v)$  is the probability of finding a particle, with mass  $m$ , having velocity  $v$  as a function of the gas temperature,  $T$ .  $k$  is the Boltzmann constant.

The initial cloud shape is shown in Figure 3.2. It has a Gaussian distribution along  $\hat{x}$ ,  $\hat{y}$ , and  $\hat{z}$  with the standard deviations given by:

$$\sigma_x = 3 \text{ mm} \quad (3.13)$$

$$\sigma_y = 10 \text{ } \mu\text{m} \quad (3.14)$$

$$\sigma_z = 10 \text{ } \mu\text{m} \quad (3.15)$$

We simulate  $10^6$  atoms while we expect to have  $10^{10}$  atoms. If the density is kept constant, increasing particle number by  $10^4$  is equivalent to increasing the volume by the same factor. As a rough approximation we can take the Gaussian standard deviations as radii of an ellipsoid. The volume of the ellipsoid is then  $4/3\pi\sigma_x\sigma_y\sigma_z$ . Scaling the volume of the ellipsoid by  $10^4$  corresponds to an

increase in  $\sigma_{y,z}$  by a factor of 100 each if  $\sigma_x$  is kept at 3 mm. Thus, with  $10^{10}$  atoms, the initial cloud shape need not necessarily be pencil-shaped. It can in fact be spherical. Having a cloud shaped like a pancake transverse to the  $z$  – *axis* would help increase the final density. This is because the hexapole trap does not act along the  $z$  – *direction* and the density along the  $z$  – *axis* remains constant.

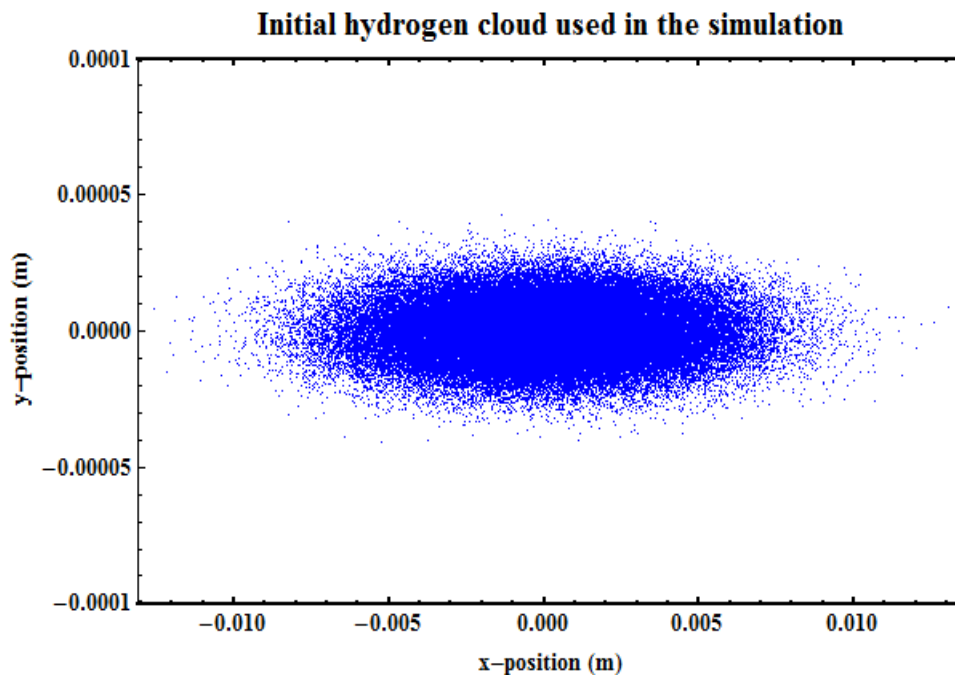


Figure 3.2: Initial cloud distribution used in our simulation. The cloud contains  $10^6$  atoms in a Gaussian profile with standard deviations given in Equations 3.13, 3.14 and 3.15. Because the magnetic hexapole does not act in the  $z$  – *direction*, the width of the cloud in the  $z$  – *direction* does not affect the results.

### 3.3 Equations of motion

The particles follow deterministic trajectories according to the classical equations of motion. We start with the Lagrangian:

$$L = T - E_{int} = \frac{1}{2}m\dot{\rho}^2 - \frac{1}{2}\mu_B\kappa\rho^2 \quad (3.16)$$

Because there is no force in the  $z$  - *direction* we can work in two dimensions, in the plane transverse to the  $z$  - *axis*. Switching to the Cartesian plane with  $\rho^2 = x^2 + y^2$  and  $\dot{\rho}^2 = \dot{x}^2 + \dot{y}^2$ , we see that motion in the equations of motion are decoupled. The one-dimensional Lagrangian for coordinate  $x_i$ , with  $i = 1, 2$ , is:

$$L = \frac{1}{2}m\dot{x}_i^2 - \frac{1}{2}\mu_B\kappa x_i^2 \quad (3.17)$$

From this Lagrangian we obtain the one-dimensional equation of motion for a harmonic oscillator:

$$\ddot{x}_i + \frac{\mu_B\kappa}{m}x_i = 0 \quad (3.18)$$

The frequency of oscillation,  $\omega$ , is easily obtained:

$$\omega = \sqrt{\frac{\mu_B\kappa}{m}} \quad (3.19)$$

The general form of the solution is:

$$x_i(t) = A\cos(\omega t) + B\sin(\omega t) \quad (3.20)$$

The parameters A and B can be found using Equation 3.20, its time derivative, and the initial conditions at time  $t = 0$ . This finally yields the result:

$$x_i(t) = x_i(0)\cos(\omega t) + \frac{v_{0i}}{\omega}\sin(\omega t) \quad (3.21)$$

where  $v_{0i}$  is the atom's initial velocity in the  $i$ 'th direction.

Each atom is propagated according to Equation 3.21 for the duration of the pulse. After a pulse of duration  $t_p$  the atoms continue to travel with a constant velocity given by:

$$v_i(t_p) = v_{0i}\cos(\omega t_p) - x_i(0)\omega\sin(\omega t_p) \quad (3.22)$$

The final density is calculated inside a sphere located at the center and having a radius  $r$ :

$$n_H = \frac{\text{atoms}}{4/3\pi r^3} \quad (3.23)$$

As mentioned in Section 3.2, we expect to have  $10^4$  more atoms than we simulate. We can expect that with more atoms the high density region has a radius that is greater than  $1 \mu\text{m}$

### 3.4 Choosing the right kick strength

What kind of hexapole field strengths do we want? If the field is too strong, the period of oscillation,  $\omega$ , given by Equation 3.19, is so small that and there is not enough time to switch the field off before the occurrence of TBA. Table 3.4 gives the time required for an atom to reach the center as a function of the field strength,  $\kappa$ , assuming the trap is on continuously. In our simulation we focus on the case where  $\kappa = 10^5$ . This is largely because we know this field strength is feasible from previous experiments [24]. Table 3.1 shows that a  $10 \mu\text{s}$  pulse is reasonable for this field strength.

Table 3.1: Values of the half-period of oscillation,  $T/2$ , as a function of the field strength constant,  $\kappa$ .

$\kappa(T/m^2)$	$10^3$	$10^4$	$10^5$	$10^6$	$10^7$
$T/2$ ( $\mu s$ )	1334.2	421.9	133.4	42.2	13.3

## 3.5 Results

We find that a 10  $\mu s$  magnetic kick from a hexapole trap effectively implodes a cloud of hydrogen and high densities in the center are reached. Below are results of a simulation run for  $10^6$  atoms given a 10  $\mu s$  kick of field strength  $\kappa = 10^5$  T/m<sup>2</sup>. The cloud is given a range of initial temperatures. The results show that inside a 10  $\mu m$  sphere, number densities of  $10^{16}$  cm<sup>-3</sup> are reached. The results are shown in Figure 3.3. Implosion happens about 177  $\mu s$  after the kick. These results have been verified by an independent simulation done by Tharon Morrison [28].

### 3.5.1 Reaction temperature

The temperature of the gas at the time of the TBA reaction is calculated using the average particle velocity,  $v_{rms}$ :

$$T = \frac{mv_{rms}^2}{k} \quad (3.24)$$

with  $m$  the mass of the hydrogen atom and  $k$  the Boltzmann constant. It is worthwhile to note that the further away from the center that an atom starts, the greater the momentum kick it will be given. Thus, if a cloud is initially

spread far out from the center, the reaction will be hotter than if the cloud was to start in a more compressed shape.

The expression for the temperature given above is an approximation because the TBA process is exothermic and heats up the gas. This is discussed further in Section 4.2. The reaction temperature depends on the momentum imparted to the atoms by the kick. Table 3.2 shows the reaction temperatures for various field strength constants and a 10  $\mu$ s kick. The initial temperature has very little effect on the reaction temperature, as the velocities the atoms obtain from the kick are much greater than the velocities of the initial thermal motion. The initial temperature does, however, have a noticeable effect on the peak density during implosion, as can be seen in Figure 3.3

Table 3.2: Reaction temperatures,  $T$ , calculated from the simulated motion of atoms at the time of implosion.  $\kappa$  is the field strength and pulse duration is assumed to be 10  $\mu$ s. The initial cloud temperature in this example is 10 nK, though the initial temperature has little effect on reaction temperature.

$\kappa$ ( $T/m^2$ )	$10^3$	$10^4$	$10^5$	$10^6$	$10^7$
$T$ (K)	$1 \times 10^{-6}$	$1 \times 10^{-4}$	$1 \times 10^{-2}$	1	10

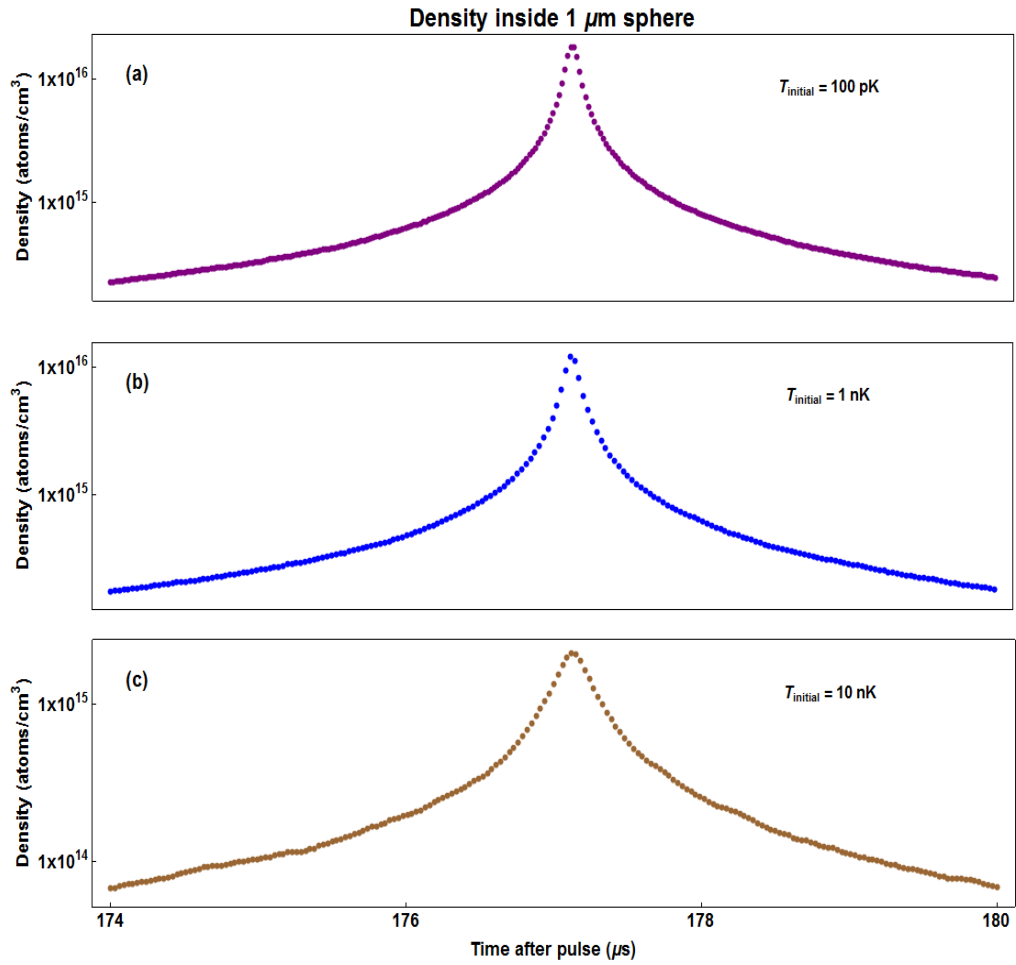


Figure 3.3: Simulated cloud densities during implosion.  $10^6$  atoms are given a  $10 \mu\text{s}$  kick with  $\kappa = 10^5 \text{ T/m}^2$ . Initial cloud temperatures are given. It can be seen that the initial cloud temperature has a significant effect on final density.

## Chapter 4

### Discussion

In our idealized point-particle simulation, we show that densities exceeding  $10^{16} \text{ cm}^{-3}$  can be achieved at the center of the hexapole trap. In this Chapter I use the published TBA rate coefficients to examine the percent conversion of hydrogen to molecular hydrogen on short time scales. Given the simulation results it appears feasible to design a hexapole trap in such a way as to observe TBA through implosion.

This simulation does not take thermodynamic, chemical, quantum, or two-body effects into account. The question of validity naturally arises. In the second half of this Chapter I focus on the most immediate of the above, which is the thermal evolution of the cloud. The TBA reaction rate depends on temperature, but the TBA process itself is exothermic. Therefore, it is expected that there is a point in the life of a hydrogen gas cloud at which it becomes unstable. I briefly discuss the expected secondary reactions. I conclude with suggestions for future work.

## 4.1 Can we achieve densities that are high enough for TBA?

If we denote the H<sub>2</sub> number density as  $n_{H_2}$  then  $\dot{n}_{H_2}$  represents the rate per volume at which H<sub>2</sub> is formed. For a monatomic three-body process, the rate of conversion is given by:

$$\dot{n}_{H_2} = n_H^3 k_3 \quad (4.1)$$

where  $n_H$  is the hydrogen atom number density and  $k_3$  is the hydrogen TBA rate constant in units of cm<sup>6</sup> s<sup>-1</sup>.

The rate constant,  $k_3$ , has been estimated by Jacobs et. al. (1967) [5], Abel et. al. (2002) [6], Flower & Harris (2007) [7] and Forrey (2013) [9]. These published rates are summarized in Table 4.1

Table 4.1: Hydrogen TBA rate constants as published by various authors. T is the gas temperature in Kelvin.

author	$k_3$ (cm <sup>6</sup> s <sup>-1</sup> )
Jacobs	$5.5 \times 10^{-29} T^{-1}$
Abel	$1.3 \times 10^{-32} (T/300K)^{-0.38}$
Flower & Harris	$1.44 \times 10^{-26} T^{-1.54}$
Forrey	$6 \times 10^{-32} T^{-1/4} + 2 \times 10^{-31} T^{-1/2}$

Figure 4.1 plots the above rate constants as a function of temperature for low temperatures. Only the rate constant published by Abel et. al. is specifically for  $T < 300$  K, though the authors do not state what the lower temperature limit is for their constant. The constants published by the other

three authors are for temperatures relevant for star formation: 200 K and up. Therefore, how valid these rate constants are for very low temperatures is unclear.

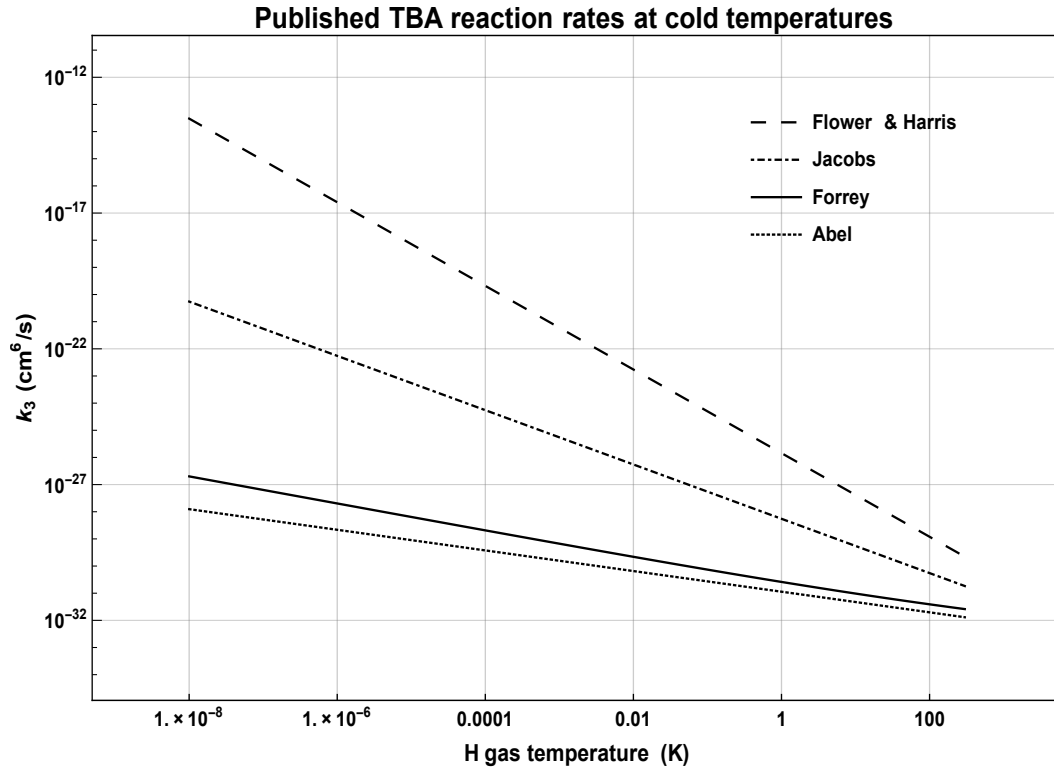


Figure 4.1: TBA rate constants based on published estimates. The constants are plotted for the temperature range: 10 nK - 300 K. The constant published by Abel is specifically for temperatures below 300 K.

#### 4.1.1 Percent conversion

Taking the results shown in Figure 3.3 we see that, starting with a cold cloud at a density of  $10^{14} \text{ cm}^{-3}$ , densities of  $10^{16} \text{ cm}^{-3}$  are attainable for

periods lasting several  $\mu\text{s}$ . Whether such high densities are actually needed is uncertain. Such high densities are a "worst case scenario," and it is in the realm of possibility that a starting density that is lower than  $n_H = 10^{14} \text{ cm}^{-3}$  is needed.

The percent conversion of H into  $\text{H}_2$  depends on the amount of time that elapses. Because the hexapole trap polarizes the hydrogen atoms, dipole interactions will prevent TBA from occurring while the atoms are accelerating toward the center. As soon as the hexapole trap is switched off, TBA will begin. It was shown [4] that all atomic hydrogen will be converted to molecular hydrogen for densities  $n_H \geq 10^8 \text{ cm}^{-3}$ , but this is if the reaction is given enough time.

According to Savin [8] the REMPI method of detection relies on a laser pulse of 10 ns duration and a 10 Hz repetition rate. Thus we want to analyze the percent conversion on time scales between 10 ns and 100  $\mu\text{s}$ . The duration of time one waits before measuring is ultimately limited by the amount of time it takes the atoms to reach the trap center. If we wait too long the atoms will cross the middle and start zooming away from the center.

I look at the percent conversion from H to  $\text{H}_2$  for times between 1 ns and 100  $\mu\text{s}$ . I use the highest rate constant, published by Flower & Harris, and the lowest rate constant, belonging to Abel et. al., as these are the two extreme cases. I use the following expression in calculating the percent conversion:

$$\% = \frac{\dot{n}_{\text{H}_2} \Delta t}{n_H} \times 100 \quad (4.2)$$

with  $\Delta t$  the elapsed time since TBA begins.

For each of the two rate constants I plot the percent conversion as a function of time for  $T = 10$  mK and  $T = 1$  K. According to the simulation, these are reasonable reaction temperatures. However, once a certain amount of the hydrogen is converted to molecular form, the energy released in forming  $H_2$  may heat the gas significantly, accelerating the TBA rate further. I do not take this possible change in temperature into account. From the plots it can be seen that the initial reaction temperature does not have a significant effect on the reaction rate, while the difference between the constants of Flower & Harris and Abel et. al. makes a significant difference to the required atom density.

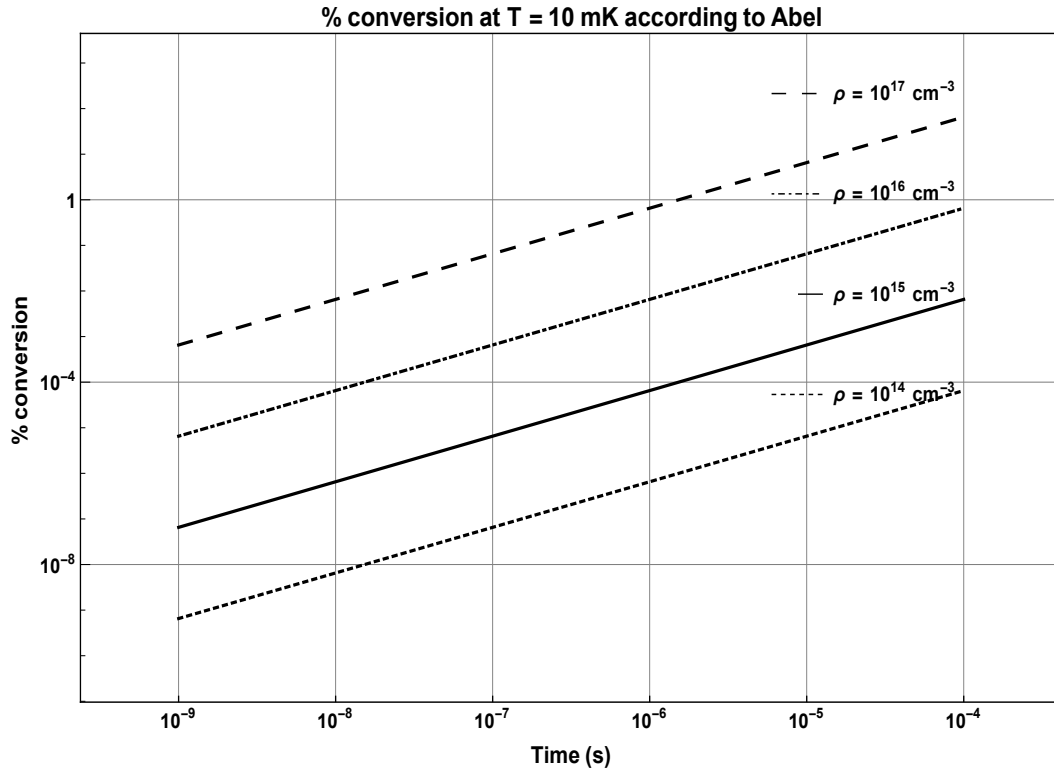


Figure 4.2: The percent conversion of H into  $\text{H}_2$  using  $k_3$  expression of Abel et. al. The reaction temperature is assumed to be 10 mK, which corresponds to a  $10 \mu\text{s}$  kick with  $\kappa = 10^5 \text{ T/m}^2$ .

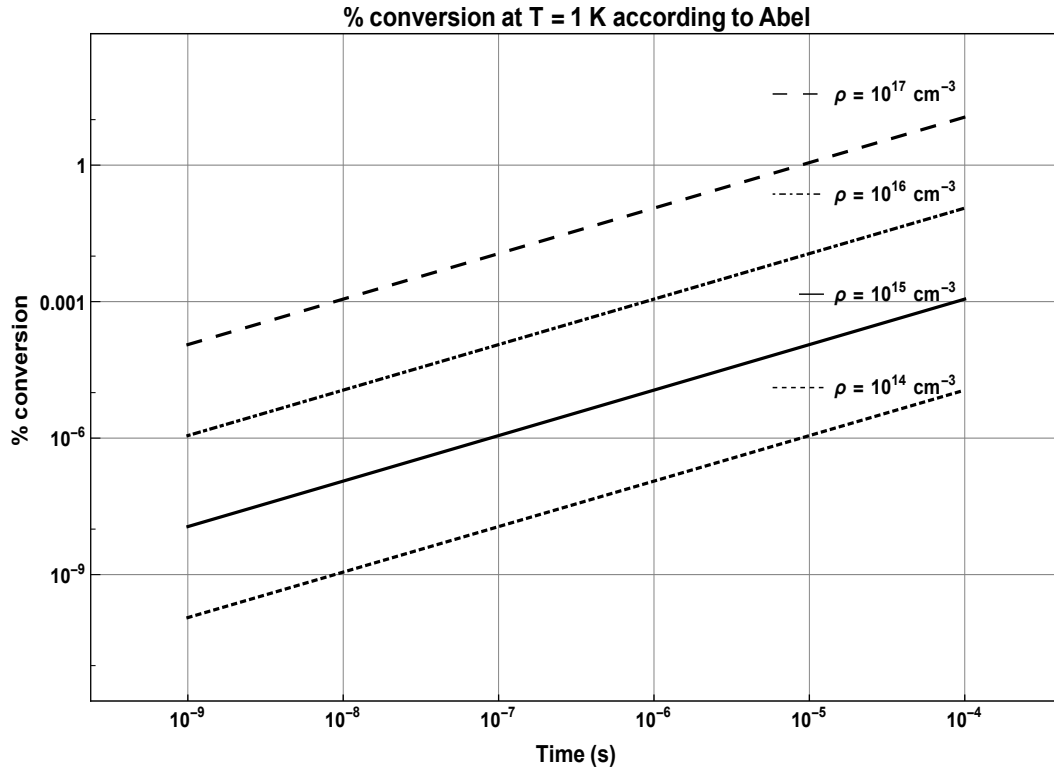


Figure 4.3: The percent conversion of H into H<sub>2</sub> using  $k_3$  expression of Abel et. al. The reaction temperature is assumed to be 1 K, which corresponds to a 10  $\mu$ s kick with  $\kappa = 10^6$  T/m<sup>2</sup>.

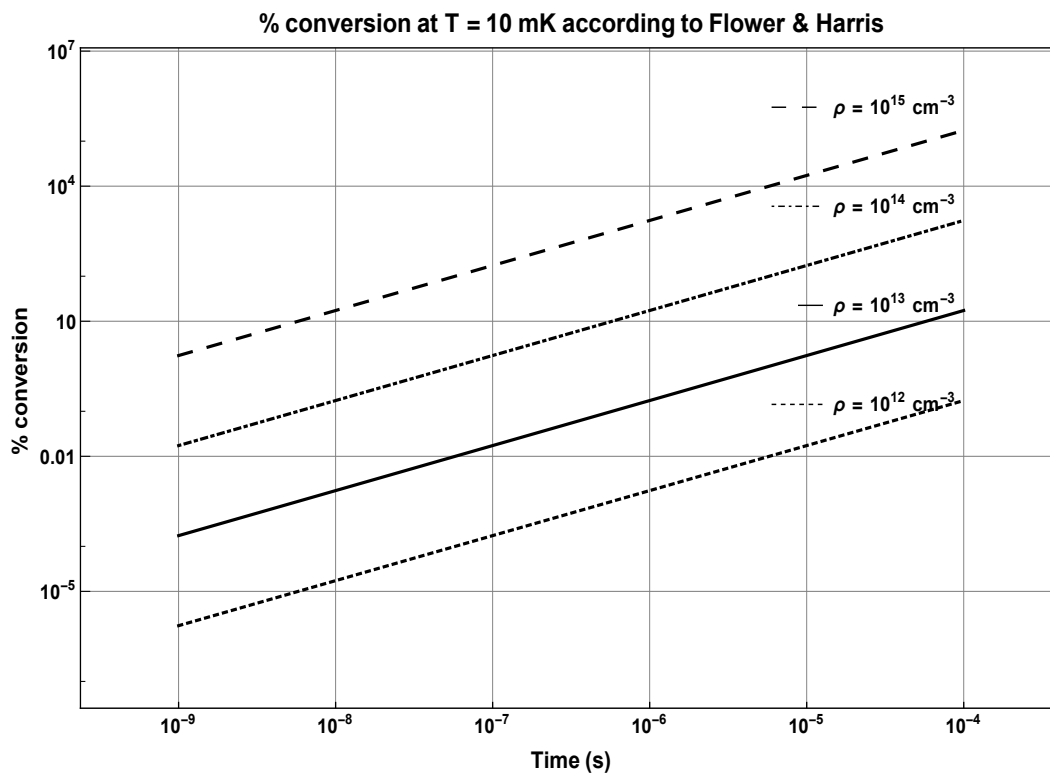


Figure 4.4: The percent conversion of H into H<sub>2</sub> using  $k_3$  expression of Flower & Harris. The reaction temperature is assumed to be 10 mK, which corresponds to a 10  $\mu$ s kick with  $\kappa = 10^5$  T/m<sup>2</sup>

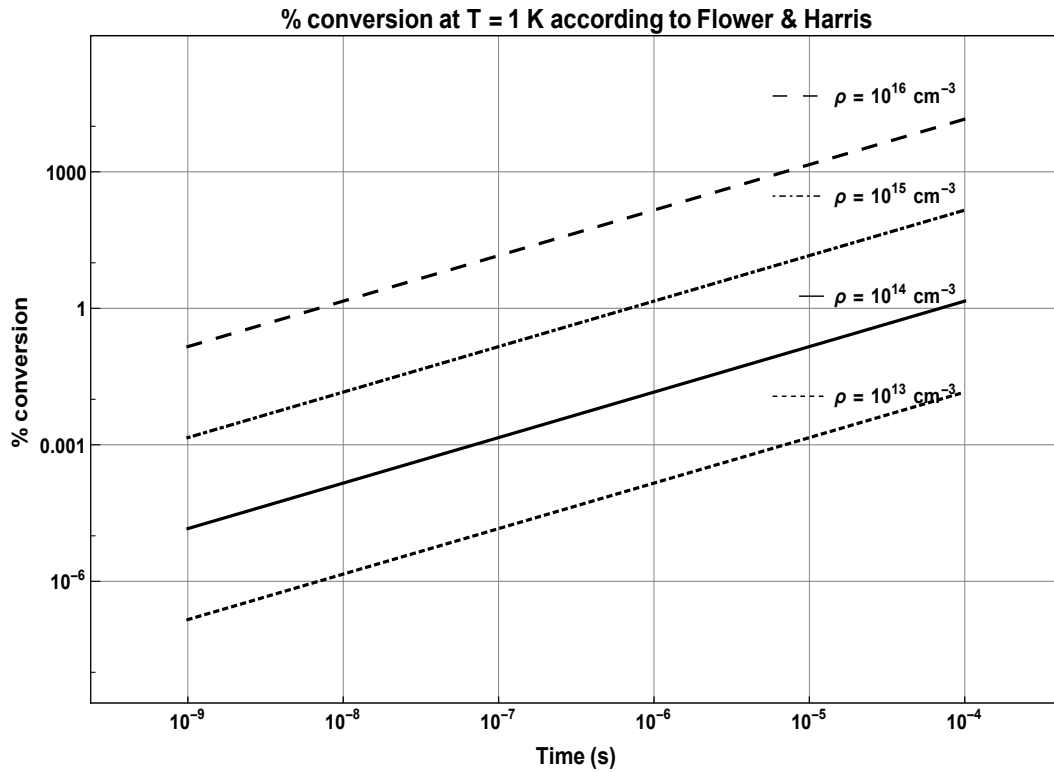


Figure 4.5: The percent conversion of H into H<sub>2</sub> using  $k_3$  expression of Flower & Harris. The reaction temperature is assumed to be 1 K, which corresponds to a 10  $\mu$ s kick with  $\kappa = 10^6$  T/m<sup>2</sup>.

## 4.2 Thermodynamics and secondary reactions

### 4.2.1 Heating

The TBA reaction is exothermic and the amount of energy released during the process corresponds to the  $H_2$  binding energy of 4.48 eV. Some of this energy goes into exciting the rotational and vibrational states of  $H_2$ , but most goes to kinetic energy. At low temperatures, the hydrogen scattering length is anomalously low at 0.648 Å. This is helpful because for a cold gas of hydrogen, the two-body elastic scattering cross-section is small.

We can approximate the heat gain from the TBA reaction with the following expression [29]:

$$\Gamma = 4.48 \text{ eV } \dot{n}_{H_2} \quad (4.3)$$

How this heat is dissipated in the cloud is not a simple question. To calculate the rise in temperature due to TBA we would need to know the specific heat of the gas. However, because as the cloud is imploding the hydrogen gas is on its way out of quantum degeneracy, this calculation is beyond the scope of this thesis.

### 4.2.2 Cooling

Once  $H_2$  is formed, other reactions can begin. There is another TBA process that can take place:



Also, collisional dissociation takes on the forms:



Reaction 4.4 becomes important only when the  $H_2$  abundance is large [7]. According to Jacobs et. al. [5] the reaction rate constant of Reaction 4.5 is smaller than  $k_3$  by a factor of 8. Similarly, the rate of Reaction 4.6 is smaller than the rate of Reaction 4.4 by a factor of 8 as well. Moreover, this applies to temperatures higher than those considered in this work. Since the dissociation temperature of molecular hydrogen is about 52,000 K, the rate coefficient for the dissociative reactions is negligible for temperatures below  $T \sim 1000$  K [7]. As long as we do not convert a significant part of the cloud to  $H_2$  we can ignore these reactions.

Prior to  $H_2$  dissociation, the cooling rate of an atomic hydrogen gas cloud is dominated by the  $H_2$  rotational and vibrational transitions [4]. We can obtain radiative cooling rates per molecule as a function of temperature in Abel et. al. The cooling rate falls off sharply for low temperatures. For the temperatures with which we are concerned the radiative loss is insignificant. Thus for the proposed experiment, cooling processes should not play a significant role.

### 4.3 Concluding remarks

In this thesis it has been shown that an atomic hydrogen cloud in an experimentally realistic, pulsed hexapole magnetic trap will implode and reach peak densities exceeding  $10^{16} \text{ cm}^{-3}$ . This indicates that the TBA of hydrogen is observable at short time scales with the range of densities that is available in the proposed experimental scheme. It has also been shown that the hexapole field strength and pulse duration, as well as the initial atom distribution, can all be used to control the final temperature and density.

For more insight into what happens to the hydrogen cloud during implosion, the effect of two-body scattering at the moment of implosion should be taken into consideration. It may also be of value to approximate the expected heat gain from the TBA reaction, and to adjust the expected TBA rate and percent conversion accordingly. This important nonlinearity in the TBA process can easily be simulated if the specific heat of the imploding hydrogen cloud is known. Further, details of the detection method will set constraints on the atom density required to observe the TBA of hydrogen.

## Bibliography

- [1] Christopher J. Foot. *Atomic Physics*. Oxford University Press, New York, 2005.
- [2] A. E. Orel. Nascent vibrational/rotational distribution produced by hydrogen atom recombination. *J. Chem. Phys.*, 87:314, 1987.
- [3] M. J. Turk et. al. Effects of varying the three-body molecular hydrogen formation rate in primordial star formation. *ApJ*, 726:55, 2011.
- [4] F. Palla, E. E. Salpeter, and Steven W. Stahler. Primordial star formation: the role of molecular hydrogen. *ApJ*, 271:632, 1983.
- [5] T. A. Jacobs, R. R. Giedt, and Norman Cohen. Kinetics of hydrogen halides in shock waves. ii. a new measurement of the hydrogen dissociation rate. *J. Chem. Phys.*, 47:54–57, 1967.
- [6] T. Abel, G. L. Bryan, and M. L. Norman. The formation of the first star in the universe. *Science*, 295:93–98, 2002.
- [7] D.R. Flower and G.J. Harris. Three-body recombination of hydrogen during primordial star formation. *MNRAS*, 377:705–710, 2007.
- [8] D.W. Savin. Laboratory measurements of primordial chemistry. *AIP Conf. Proc.*, 1480:81–86, 2012.

- [9] Robert C. Forrey. Rate of formation of hydrogen molecules by three-body recombination during primordial star formation. *Astrophys. J. Lett*, 773:L25, 2013.
- [10] D. A. Bell, H. F. Hess, G. P. Kochanski, S. Buchman, L. Pollack, Y. M. Xiao, D. Kleppner, and T. J. Greytak. Relaxation and recombination of spin-polarized atomic hydrogen. *Phys. Rev. B*, 34:7670, 1986.
- [11] H. F. Hess, D. A. Bell, G. P. Kochanski, D. Kleppner, and T. J. Greytak. Temperature and magnetic field dependence of three-body recombination in spin-polarized hydrogen. *Phys. Rev. Lett*, 52:1520, 1984.
- [12] S. G. Karshenboim, F. S. Pavone, G. F. Bassani, M. Inguscio, and T. W. Hänsch. *The Hydrogen Atom: Precision Physics of Simple Atomic Systems*. Springer, 2001.
- [13] V. Zehnlé and Jean Claude Garreau. Continuous-wave doppler cooling of hydrogen atoms with two-photon transitions. *Phys. Rev. A*, 63, 2001.
- [14] I. F. Silvera and J. T. M. Walraven. Stabilization of hydrogen at low temperature. *Phys. Rev. Lett.*, 44:164, 1980.
- [15] T. J. Greytak and D. Kleppner. Lectures on spin-polarized hydrogen. In G. Grynberg and R. Stora, editors, *New Trends in Atomic Physics*. North Holland, Amsterdam, 1984.
- [16] Harald F. Hess. Evaporative cooling of magnetically trapped and compressed spin-polarized hydrogen. *Phys. Rev. B*, 34:3476, 1986.

- [17] H. F. Hess, G. P. Kochanski, J. M. Doyle, N. Masuhara, D. Kleppner, and Thomas J. Greytak. Magnetic trapping of spin-polarized atomic hydrogen. *Phys. Rev. Lett.*, 59:672, 1987.
- [18] N. Masuhara, J.M. Doyle, J.C. Sandberg, D. Kleppner, T. J. Greytak, H.F. Hess, and G.P. Kochanski. Evaporative cooling of spin-polarized atomic hydrogen. *Phys. Rev. Lett.*, 61:935, 1998.
- [19] D. G. Fried, T. C. Killian, L. Willmann, D. Landhuis, S. C. Moss, D. Kleppner, and T. J. Greytak. Bose-einstein condensation of atomic hydrogen. *Phys. Rev. Lett.*, 81:3811, 1998.
- [20] E. Narevicius and Mark G. Raizen. Toward cold chemistry with magnetically decelerated supersonic beams. *Chem. Rev.*
- [21] R. Côté, M. J. Jamieson, Z-C Yan, N. Geum, G. H. Jeung, and A Dalgarno. Enhanced cooling of hydrogen atoms by lithium atoms. *Phys. Rev. Lett.*
- [22] M. G. Raizen, D. Budker, S. M. Rochester, J. Narevicius, and E. Narevicius. Magneto-optical cooling of atoms. *Opt. Lett.*
- [23] E. A. Hinds and I. G. Hughes. Magnetic atom optics: mirrors, guides, traps, and chips for atoms. *J. Phys. D: Appl. Phys.*, 32:R119, 1999.
- [24] R. Castillo-Garza, J. Gardner, S. Zisman, and Mark G. Raizen. Nanoscale imaging of neutral atoms with a pulsed magnetic lens. *ACS Nano*, 7:4378, 2013.

- [25] Adam Libson. *General Methods of Controlling Atomic Motion: Experiments with Supersonic Beams as a Source of Cold Atoms*. PhD thesis, The University of Texas at Austin, 1981.
- [26] K.-D. Rinnen, M. A. Buntine, D. A. V. Kliner, and Richard N. Zare. Quantitative determination of  $\text{h}_2$ ,  $\text{hd}$ , and  $\text{d}_2$  internal-state distribution by (2+1) resonance-enhanced multiphoton ionization. *J. Chem. Phys.*, 95:214, 1991.
- [27] Greg. O. Sitz. private communication.
- [28] Tharon Morrison. *Hydrogen studies including simulations for three-body association and development of in-situ silicon passivation*. PhD thesis, The University of Texas at Austin, 2014.
- [29] N. Yoshida, K. Omukai, L. Hernquist, and Tom Abel. Formation of primordial stars in a  $\lambda$  cdm universe. *ApJ*, 652, 2006.
- [30] M. J. Jamieson, A. Dalgarno, and M. Kimura. Scattering lengths and effective ranges for he-he and spin-polarized h-h and d-d scattering. *Phys. Rev. A*, 51:2626–2629, 1994.
- [31] Frank Y.-H. Wang. Specific heat of an ideal bose gas above the bose condensation temperature. *Am. J. Phys.*, 72:1193, 2004.